Atomic force microscopy of parallel DNA branched junction arrays

Ruojie Sha [1], Furong Liu [1], David P Millar [2] and Nadrian C Seeman [1]

Background: The four arms of the Holliday junction are known to stack in pairs forming two helical domains whose orientations are antiparallel, but twisted positively by about 60°, based on electrophoretic, FRET and AFM measurements. Recent gel retardation studies suggest that a bowtie junction (containing 5′,5′ and 3′,3′ linkages in its crossover strands) may adopt a parallel conformation.

Results: An AFM study of two-dimensional arrays produced by parallelograms of bowtie junctions shows that the angle between helical domains is in the range of $-68 \pm 2°$. We demonstrate by AFM that the domains are parallel by constructing V-shaped structures whose arms are separated by $\sim 68°$ and $\sim 112°$.

Conclusions: The arms of the bowtie junction are parallel rather than antiparallel. The parallel or antiparallel nature of the junction apparently is determined by the local structure of the junction, but the sign of the angle appears to be a consequence of interarm electrostatic interactions.

[1]Department of Chemistry, New York University, New York, NY 10003, USA
[2]Department of Molecular Biology, Scripps Research Institute, 10550 N. Torrey Pines Road, La Jolla, CA 92037, USA

Correspondence: Nadrian C Seeman
E-mail: ned.seeman@nyu.edu

Keywords: Atomic force microscopy; Branched DNA; DNA parallelogram array; Holliday junction structure; 3,3′ and 5′,5′ Nucleotide linkage

Received: **10 May 2000**
Revisions requested: **13 July 2000**
Revisions received: **27 July 2000**
Accepted: **2 August 2000**

Published: **18 August 2000**

Chemistry & Biology 2000, **7**:743–751

1074-5521/00/$ – see front matter

PII: S1074-5521(00)00024-7

Introduction

The Holliday [1] junction is the most prominent DNA intermediate in genetic recombination. It is known to be involved in site-specific recombination [2–4], and it is likely to be involved in homologous recombination. The Holliday junction consists of four strands of DNA that are paired into four double helical arms flanking a branch point. This branch point typically is flanked by regions of dyad (homologous) sequence symmetry; this symmetry enables the branch point to relocate through an isomerization known as branch migration (e.g., [5]). Much of our information about the physical properties of branched junctions [6,7] derives from the study of immobile DNA branched junctions [8]; these are synthetic four-stranded complexes in which the sequence symmetry has been eliminated, thereby fixing the site of the branch point. In the accepted structural model for the immobile junction in solution, pairs of adjacent arms stack to form two helical domains [9]. This structure leads to a molecule in which two 'helical' strands have a structure similar to strands in conventional DNA double helices, and the other two 'crossover' strands connect the domains. The helical domains are oriented about +60° from antiparallel (a 60° right-handed twist) to each other; this feature has been established by fluorescence resonance energy transfer (FRET) [10], time-resolved (tr) FRET [11] and by examination of two-dimensional arrays using atomic force microscopy (AFM) [12]. Recent crystal structures confirm the key features of this model [13–15]. The definition of its parallel and antiparallel orientations is shown as a function of the orientation of the helical strand of the rear helix in Figure 1a: those conformations where its 5′ end is in the upper two quadrants are in the parallel range, and those where it is in the lower quadrant are in the antiparallel range. The antiparallel nature of the junction is somewhat puzzling, because antiparallel helix axes are not in line with models of recombinational intermediates derived from genetic experiments: homologous nucleotides are in proximity to each other only near the branch point, which is counterintuitive for systems where DNA–DNA recognition is expected to occur through interactions of homologous nucleotides.

Recently, we have explored the origin of the antiparallel structure of the Holliday analog by means of bowtie junctions [16]. These are Holliday junction analogs in which the helical strands are conventional molecules containing 5′,3′ linkages, but one crossover strand contains a 5′,5′ linkage and the other contains a 3′,3′ linkage (Figure 1b). The crossover structure of the parallel bowtie junction structure is similar to the crossover structure of the antiparallel conventional junction and vice versa, as shown in Figure 1c: from this diagram it is evident that for both molecules neither strand passes in front of the other at

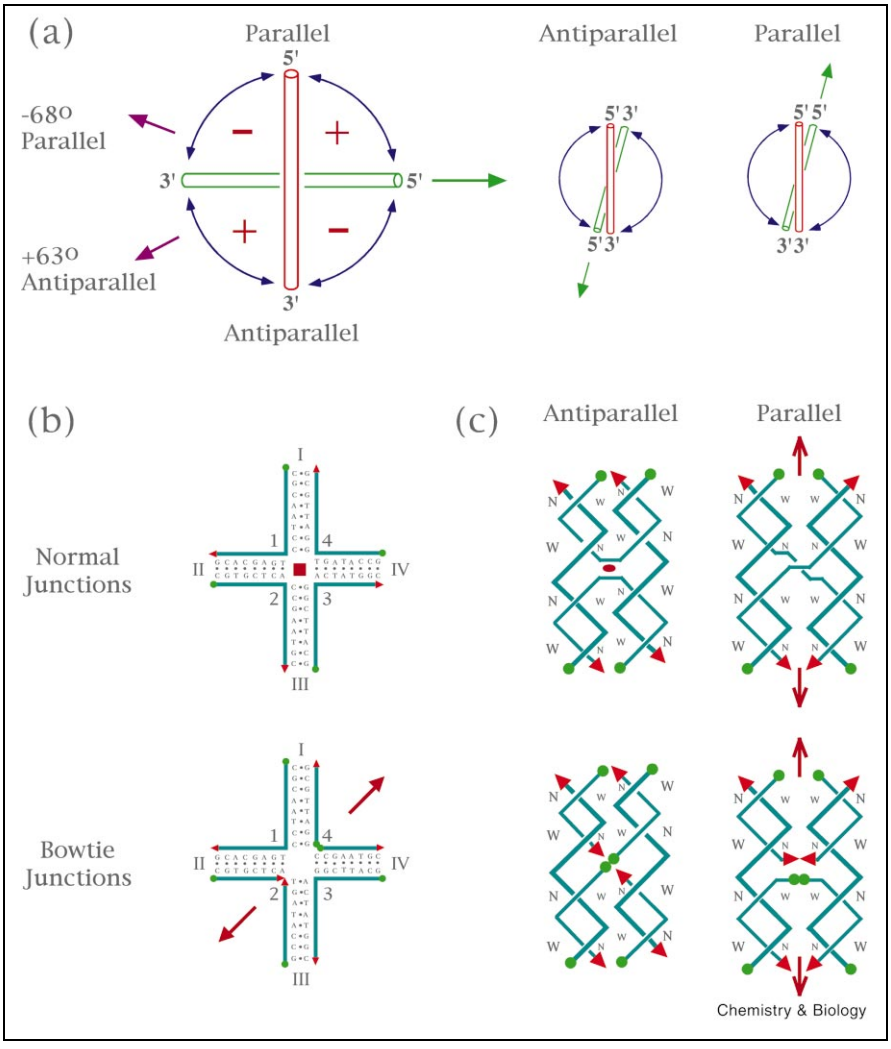

Figure 1. Conventional and bowtie branched junctions. **(a)** Conformational sign conventions. On the left, a view of a Holliday junction is shown down the axis connecting the double helical domains; yet perpendicular to both; the red vertical domain lies above the plane of the page, closer to the reader, and the green horizontal domain lies below it, further from the reader. In line with previous treatments [10], the rear domain rotates; its 5′ end is imagined to be coupled to the green arrow pointing right on the horizontal axis. When the 5′ end is above the horizontal, the structure is qualitatively 'parallel', and when it is below the horizontal, it is qualitatively 'antiparallel'. The signs of the angles are illustrated in the four quadrants; thus, if the arrow were pointing in the upper right quadrant, the conformation would be positive-parallel, in the upper left, negative-parallel, the lower left, positive-antiparallel, and the lower right, negative-antiparallel. Two particular structures are indicated on this drawing by purple arrows: +63° antiparallel corresponds to the conformation of the conventional Holliday junction [12], and −68° parallel corresponds to the conformation of the bowtie junction, as determined here. At the right of the larger diagram, two smaller diagrams are shown, illustrating the nearly ideal antiparallel and parallel structures. They are placed directly above the parallel and antiparallel schematics in **(c)**; for clarity, they have been rotated 15° into the positive quadrants from purely antiparallel or parallel. **(b)** Schematic drawings. The upper drawing shows the well-characterized immobile branched junction, J1, composed of four conventional strands of DNA. The strands are labeled with Arabic numerals and the double helical arms with Roman numerals. The 5′ ends of strands are indicated by filled green circles, and the 3′ ends are indicated by red arrowheads. Unlike a Holliday junction, there is no two-fold sequence symmetry at the branch point, so the position of the crossover cannot relocate through branch migration. The potential fourfold symmetry of the backbone is indicated by the filled brown square at the center of the branch point. The lower drawing shows the same junction converted to a bowtie junction. The sequences of strands 1 and 3 have been retained. Strand 2 now has two 5′ ends and a 3′,3′ linkage at the branch point; likewise, strand 4 has two 3′ ends, and a 5′,5′ linkage at the branch point. The unusual linkages restrict the bowtie junction backbone to twofold symmetry, about the axis indicated by two brown arrows on the diagonal. **(c)** Conformations of conventional and bowtie junctions. The same conventions apply as in **(b)**. This view corresponds to looking down the horizontal direction of **(a)**, where the rear helix has been rotated to be ideally parallel or antiparallel. The top panel shows the strand structures of the antiparallel (left) and parallel (right) conventional branched junction if its arms stack to form two helical domains. The helical strands [strands 1 and 3 of **(b)**] are drawn with a thick line, and the crossover strands [strands 2 and 4 of **(b)**] are drawn with a thin line. Major (wide) and minor (narrow) grooves are indicated by 'W's and 'N's, respectively, on both sides of each helical domain; the abutting surface on the inside of the molecule has smaller characters for reasons of clarity. Note that the major groove abuts a minor groove in the antiparallel junction, but that minor grooves abut minor grooves and major grooves abut major grooves in the parallel junction. There is a dyad axis normal to the page in the antiparallel structure, indicated by the brown lens-shaped figure at its center. The dyad axis of the parallel conformation lies in the plane of the page, and is indicated by the two brown arrows at the center. The bottom panel shows bowtie junctions drawn the same way. There is a dyad axis normal to the antiparallel bowtie junction at its center, but it has been omitted for clarity. The parallel bowtie junction has a branch point structure similar to the antiparallel conventional junction in this projection.

the crossover point in this projection; this structure contrasts dramatically with the parallel conventional junction and the antiparallel bowtie junction, where nodes are visible at the crossovers. The bowtie system allowed us to establish that interarm electrostatics appear to play a lesser role in the preference for the qualitative orientation (parallel range vs. antiparallel range) than branch point structural preferences: as assayed by gel retardation [17], the bowtie junction appears to adopt a parallel conformation, rather than an antiparallel conformation [16]. tr-FRET methods confirm this unexpected result (E. Chapman, R.S., D.P.M. and N.C.S., submitted for publication).

We have developed an AFM methodology to observe branched junctions directly in periodic arrays [12]. This method entails combining four (conventional) branched junctions (Figure 2a) into a parallelogram-like structure, as shown in Figure 2b. The structure is not really planar, because the axes of the two red parallel helical edges are designed to lie in one plane and those of the blue edges lie in a plane about 2 nm behind it. Only the crossover points of the junctions are expected to be roughly coplanar. Each helix terminates in a set of sticky ends, so it is possible to direct the parallelograms to self-assemble into one-dimensional (Figure 2c) or two-dimensional (Figure 2d) periodic arrays. The angle between the edges of the parallelograms is the angle between the helical domains of the Holliday junction, so AFM observation of the array and its autocorrelation pattern permits direct observation of the inter-domain angle in an unstressed system [12].

Here, we have applied this new approach to the analysis of bowtie junctions. We have designed and formed a pair of two-dimensional arrays from bowtie junctions, and the use of these arrays permits us to measure directly the angle between the helical domains of the bowtie junction. We can also establish the sign of the angle directly from these AFM observations. However, it is not possible to identify which arms contribute to the angle from analysis of two-dimensional arrays alone. To accomplish this task, we have attached one-dimensional reporter arrays to a single parallelogram containing sticky ends on only one adjacent pair of edges; V-shaped figures result from this self-assembly. The angles observed between the arms of the V-shaped figures establish unambiguously the parallel nature of the bowtie junction.

Results

Two-dimensional arrays of bowtie junction parallelograms

Figure 2d illustrates that a parallelogram can form an array with two different spacings, one corresponding to the area enclosed within the parallelogram, and the other corresponding to the inter-parallelogram spacing. We have used the same rhombus for both of the two-dimensional studies performed here, but the inter-rhombus spacing has been varied. The intra-rhombus spacing is four turns of

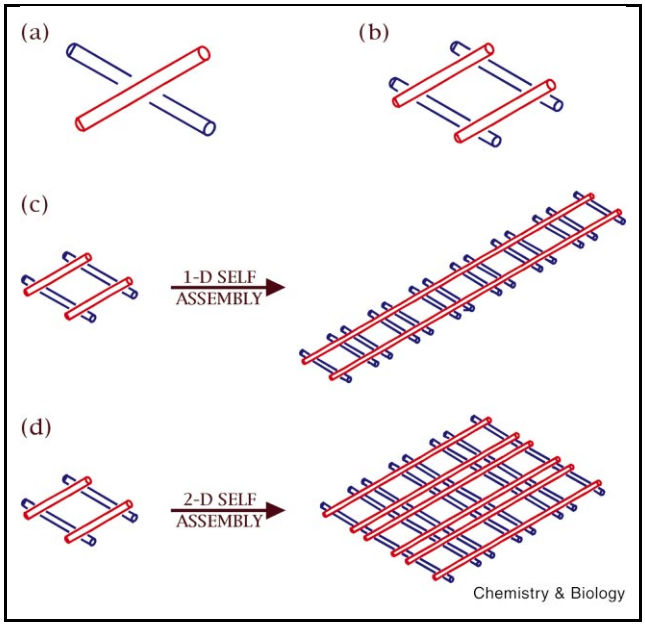

Figure 2. Constructs built from conventional junctions. **(a)** A conventional junction. A two-domain junction is shown, with the red domain closer to the reader than the blue domain. The angle between the domains is about +60°, in agreement with previous studies [10–12]. **(b)** A parallelogram built from four junctions. Four junctions of the type shown in **(a)** are shown combined into a parallelogram. The red edges are about 2 nm closer to the reader than the blue edges. This particular parallelogram is equilateral. **(c)** A one-dimensional array built from DNA parallelograms. The red edges have been connected by sticky-ended self-association to produce a railroad-like arrangement. The separation of the blue 'ties' is shorter between parallelograms than within them. **(d)** A two-dimensional array build from DNA parallelograms. In this case, the parallelogram has self-associated in two dimensions to form an array. All of these structures have been reported previously [12].

DNA, and the inter-rhombus spacing of the first array is two turns of DNA (called a 4+2×4+2 motif), for a six-turn periodicity, as shown in Figure 3a. The upper left panel shows the array in full, the upper middle shows a zoom, the upper right shows a Fourier-smoothed image of the zoom, and the lower left contains its autocorrelation function. As noted previously [12], the two-turn spacing is not resolved readily; the knobs visible in the image correspond to the small rhombus figures in Figure 2d. The autocorrelation function demonstrates clearly that the angle between the helical domains is 67°, and that the spacings observed are very close to those predicted. Likewise, it is clear from this image that the sign of the angle is negative, because one direction clearly is lying over the other one. This sign is opposite from that seen for Holliday junctions composed of conventional strands. The position is indicated by the arrow in Figure 1a.

The array in Figure 3b is an array in which both the intra-

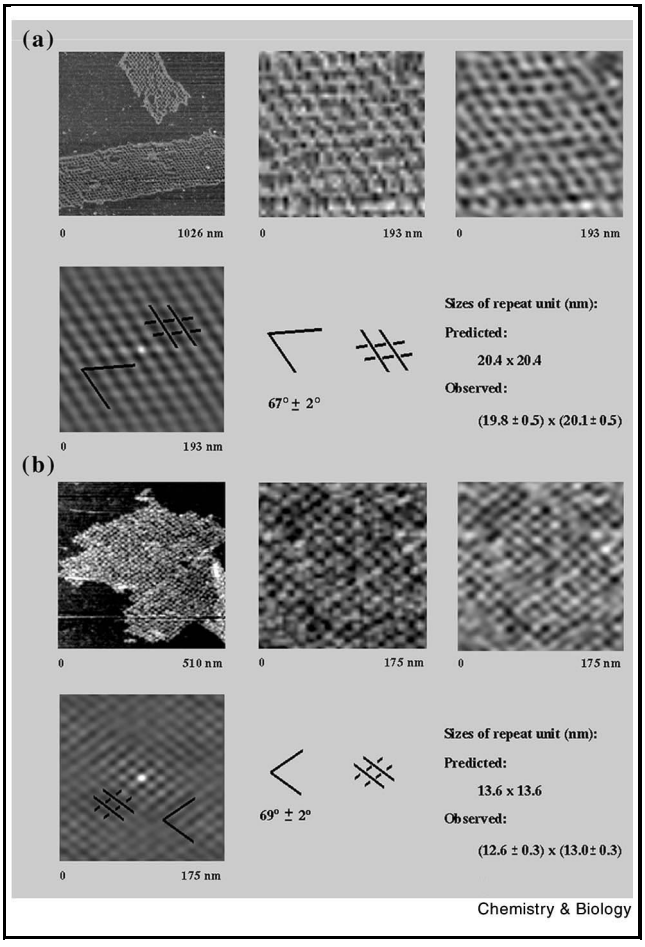

Figure 3. Two-dimensional arrays of bowtie parallelograms. **(a)** 4+2×4+2 arrays. The upper left panel shows a distant view of an array, the upper center panel shows a zoom, the upper right panel illustrates a Fourier smoothing of the upper center, and the lower left panel shows the autocorrelation function of the upper right. The knobs visible in the upper right panel correspond to the small rhombi of the bowtie version of Figure 2d, which are not resolved. The angle between domains is emphasized in the lower left, and is re-drawn in the lower center. The sign of the angle is evident in the autocorrelation function, because one set of domains clearly is in front of the other. The predicted and observed periodicities in the autocorrelation function are indicated. **(b)** 4+4×4+4 arrays. The same conventions apply as in **(a)**. The knobs now correspond to single intersections. The sign of the angle is less clear in the autocorrelation function, possibly because the array is less robust to contact mode scanning. The periodicity indicated is the half-periodicity of the individual repeat; the actual chemical periodicity is twice that indicated.

rhombus spacing and inter-rhombus spacing are four turns of DNA (a 4+4×4+4 motif). Hence, the apparent periodicity is smaller, four turns of DNA, although the true periodicity is eight turns of DNA. The knobs in the zoom are smaller, because they correspond only to the crossings of two helices, not four. The angle between helices in this array is similar to that in the other array, 69°. The agreement between predicted and observed spacing is good. The sign of the angle is somewhat ambiguous in this image. The cause of this ambiguity may be that each streak consists of two helices in Figure 3a, but they consist of only a single helix here, and therefore are more susceptible to perturbations from AFM scanning in contact mode.

V-shaped arrays establish the parallel nature of the bowtie junction

The AFM characterization of bowtie junctions would be incomplete if we could not ascertain unambiguously that the parallel structure produces the features noted above. The low resolution of the AFM necessitates the use of an amplification technique. It is important to realize that both the parallel and the antiparallel structures are distorted quite far from their ideals of 0° and 180°. The angle determined for the conventional antiparallel junction is 63.5° [12], and the angle determined here for the bowtie junction is about −68°. Figure 1a shows that we are asking about a difference of roughly 50°. The exact question being asked is shown graphically at the top of Figure 4a. The left structure is parallel, and the right structure is antiparallel, drawn within the twisted context described above. The distinction between these two structures is the angle that encloses the unusual linkages: on the left it is ∼68°, and on the right it is ∼117°.

It is possible to determine which of these angles is correct, because we can design molecules in which it is clear which angle encloses the unusual linkages. We have built four parallelograms of the 4+2×4+2 motif, drawn in dark blue, and labeled I, II, III and IV in Figure 4a. The letters A, B, C and D represent sticky ends, A′, B′, C′ and D′ represent their complements, respectively, and 0 represents hairpins that terminate double helical arms. Molecule I is a V-fulcrum, with hairpins on the top two edges, and sticky ends on the bottom two edges. Molecule II is also a V-fulcrum, but its hairpins are on the right, and its sticky ends are on the left. Molecules III and IV are extender parallelograms, with hairpins on one pair of opposite sides, and complementary sticky ends on the other pair of opposite sites. The combination of a single copy of molecule I, and multiple copies of molecules III and IV would lead to the sharp V-structure shown in dark blue on the left of Figure 4b. Similarly, the analogous combination of molecules II, III, and IV would lead to the blunt V-structure shown in dark blue on the right of Figure 4b.

The molecules drawn in dark blue represent the conformation that the parallelograms would assume if the helices linked by the unusual linkages were parallel, corresponding to the left structure at the top of Figure 4a. However, this is what we are trying to ascertain, not something known ahead of time. It is possible that the conformation corresponds to the molecule on the right, at the top of Figure 4a. If so, the shapes of molecules I, II, III and IV

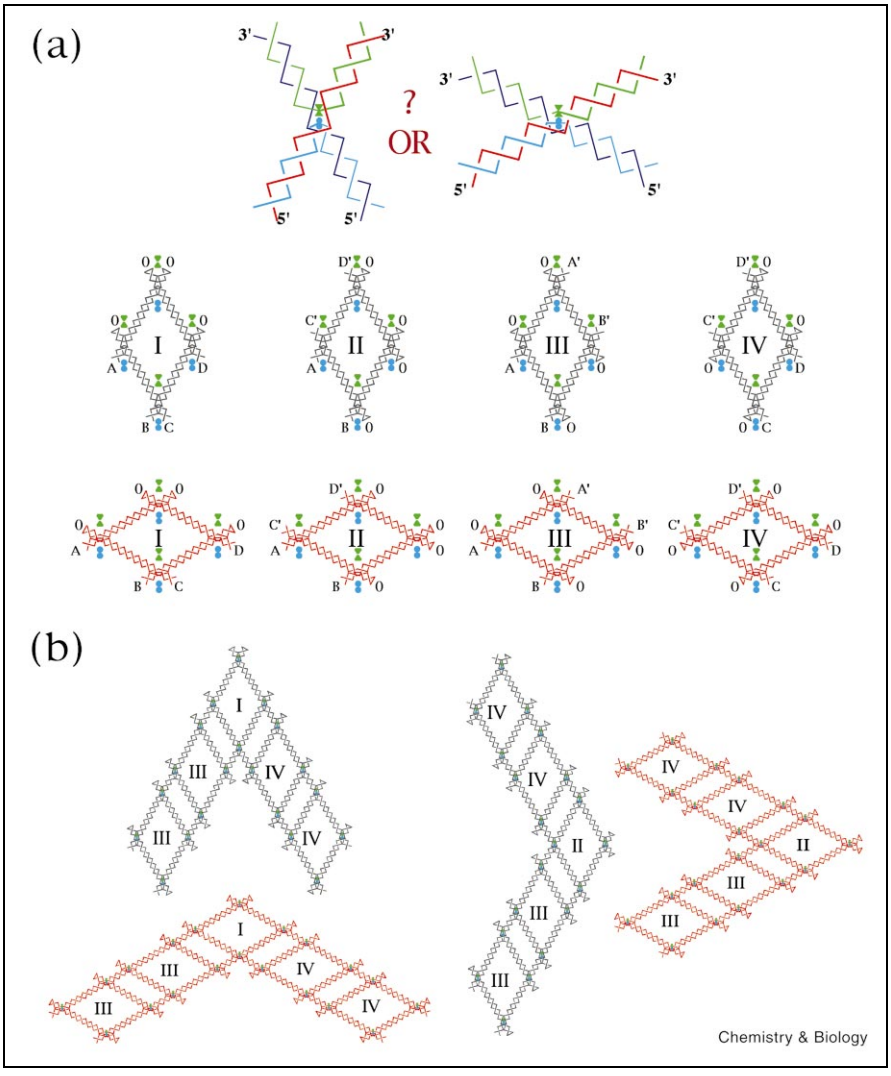

Figure 4. Schematic diagram representations of the experiment to demonstrate the parallelism of the bowtie junction. **(a)** The question and the components. The top portion shows a drawing of the bowtie junction in the parallel conformation (left) and the antiparallel conformation (right). The 5′ and 3′ ends of the helical strands are labeled. The 3′,3′ linkage is indicated by the pair of green opposed triangles, and the 5′,5′ linkage is indicated by the pair of juxtaposed blue circles. The central row shows four 4+2×4+2 rhombus figures drawn dark blue in the shape corresponding to the parallel conformation at the top left. The opposed triangle and juxtaposed circle convention is repeated here, but the symbols are removed from the strands for clarity. The figures are labeled with Roman numerals, I, II, III and IV, and the ends of their helices are labeled 0, to represent hairpins, or the letters A, B, C and D, to represent sticky ends, or A′, B′, C′ and D′ to represent their complements, respectively. The bottom row shows the same figures, but now drawn red in the antiparallel conformation of the upper right. **(b)** V-shaped arrays formed by combinations of the components in **(a)**. The left side shows the V-shaped arrays that would be formed by the combination of parallelograms I, III and IV. The acute dark-blue V-shaped figure corresponds to the parallel structure and the obtuse red V-shaped figure corresponds to the antiparallel structure. The right side shows the V-shaped arrays that would be formed by the combination of parallelograms II, III and IV. The obtuse dark-blue V-shaped figure corresponds to the parallel structure and the acute red V-shaped figure corresponds to the antiparallel structure.

would be those drawn in red, at the bottom of Figure 4a. If that were the case, the combination of molecules I, III and IV would lead to the blunt red V-structure shown in Figure 4b, and the combination of molecules II, III and IV would produce the sharp red V-structure in Figure 4b. Thus, the two possibilities are easy to differentiate.

The results of these experiments are shown in Figure 5. Figure 5a contains six AFM images of the assembly built from molecules I, III and IV. In each instance, the angle seen is in the range of 65–69°, consistent with the parallel conformation, shown in dark blue in Figure 4. This result is confirmed by the other V-shaped array, shown in Figure 5b. Here, we see six AFM images of the assembly built from molecules II, III and IV. The prediction in Figure 4b is that a parallel conformation leads to a blunt array, rather than a sharp one. It is evident that the angles of these V-shaped assemblies are in the range of 110–115°, in agreement with the dark blue structures on the right of Figure 4b. A key control for this system is the behavior of the individual components of these arrays. Figure 5c shows that these molecules by themselves do not form the structures seen in Figure 5a,b. As expected, molecules III and IV form short linear species, similar to those seen previously [12], but no V-shaped species are seen in any of the panels of this figure.

Discussion

The use of AFM to characterize macromolecular structures

We have shown that it is possible to analyze bowtie junctions by AFM in two-dimensional arrays in the same way

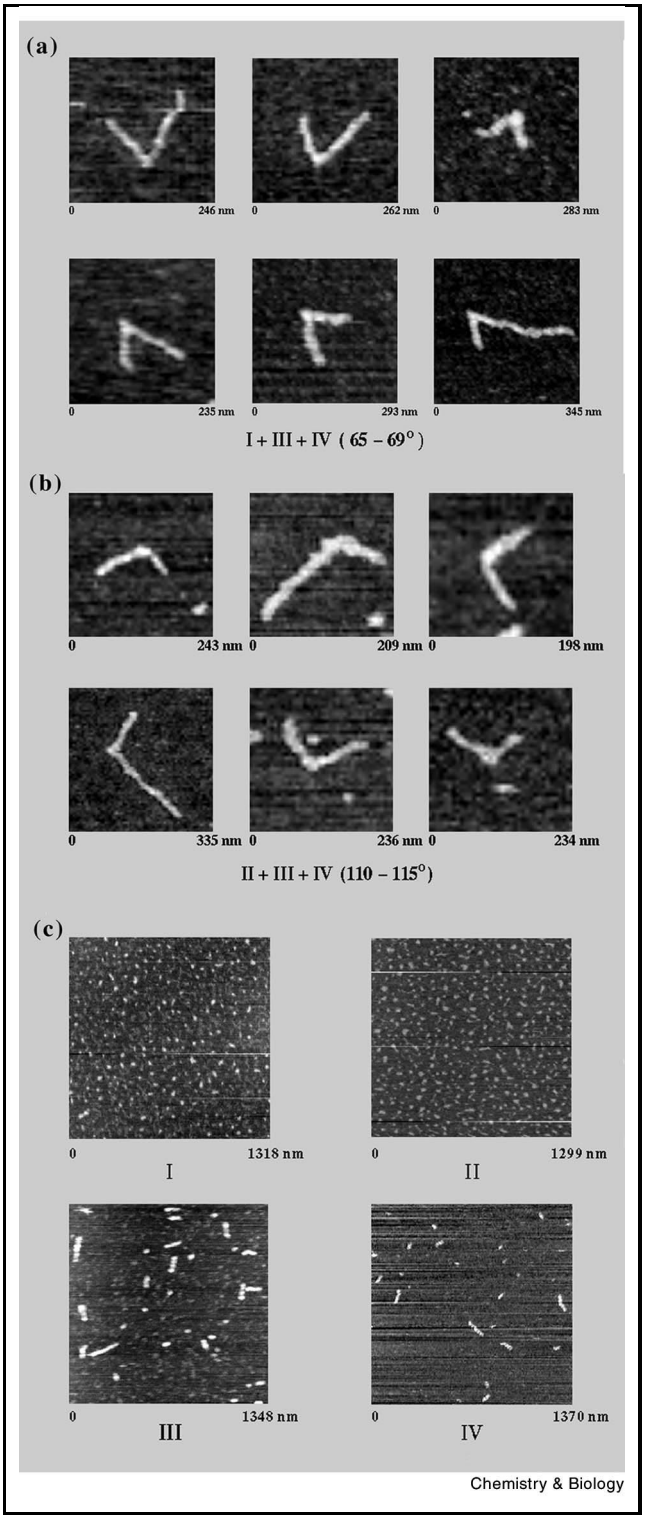

Figure 5. AFM images of the V-shaped arrays formed by bowtie parallelograms. **(a)** V-shaped arrays formed by combining parallelograms I, III and IV. All arrays have angles in the range 65–69°, in agreement with a parallel structure. **(b)** V-shaped arrays formed by combining parallelograms II, III and IV. All arrays have angles in the range 110–115°, again in agreement with a parallel structure. **(c)** Control images of individual components. The panels are labeled by the component visualized there. Little structure is shown for components I and II, and components III and IV form the linear arrays expected for them. ←

that we analyzed conventional junctions [12]. A critical control in this system is to ask whether the mica substrate influences the structure in some way. Consequently, we performed the same experiment on graphite, and obtained the same structures (data not shown). Mica is a much more convenient substrate, because DNA adheres to it more strongly, but it is possible to perform the observation on graphite.

It is clear that an approach that is taxed in delivering 7 nm resolution cannot be expected to produce high resolution information about the molecular features of individual molecules. Nevertheless, the use of 2D arrays has permitted us to establish clearly the angles between unperturbed Holliday analogs, including their signs. We tried unsuccessfully to develop a labeling scheme for the helical strands that entailed a topographic label [18–20] for marking features in a 2D array. This failure is what led us to develop the V-shaped array system used successfully here. The V-shaped array is a special example where extensive synthetic work can be used to overcome a failure of the naive use of the AFM. Thus, amplification of features in two dimensions to produce periodic systems provides recognizable data through autocorrelation and Fourier smoothing; likewise, amplification in one dimension has enabled us to distinguish two clear alternatives regarding the angles that flank the unusual linkages. These methods are likely to facilitate the characterization of similar nucleic acid systems.

Domain orientation in Holliday junction analogs

The data presented above solidify the inferences derived previously from gel retardation [16] and tr-FRET experiments: the bowtie junctions are parallel, rather than antiparallel. There is a precedent for parallel molecules in RNA junctions [21], but no parallel DNA junction has been reported unless it has been constrained within a tethered [22] or double crossover [23] molecule. Double crossover molecules constrained to contain parallel double helical domains are often ill-behaved, forming multimers visible on non-denaturing gels [23].

The structural data provided by the studies performed here help to explain the nature of the parallel structure and its origins. Although the conformation falls in the upper half of Figure 1a, we observe a parallel structure that is far from ideal. Indeed, it is nearly 70° from ideal parallelism, just as the antiparallel structure is over 60° from ideal antiparallelism. As seen in Figure 1c, the junction structure in the parallel bowtie junction qualitatively

resembles the junction structure of the antiparallel conventional junction, so it seems likely that rough domain orientation is determined by the local preferences for the crossover structure, rather than inter-domain electrostatics.

Nevertheless, electrostatics do play a role in the determination of the structure. The deviation of the helix axes from planarity, and the sign of that angle are certainly affected strongly by inter-domain electrostatics. Von Kitzing et al. [24] have shown this for the conventional branched junction, and it is evident from simple molecular model building [25] that the sign of the parallel bowtie junction is certainly determined by the inter-domain electrostatic clashes: reversing the sign leads to a structure that has numerous unfavorable interactions between backbone atoms on the two domains.

Components of biological structure

The antiparallel structures determined for Holliday junction analogs have posed a major problem for combining solution physical chemistry with genetic inferences. Homologous sequences in two chromosomes are in proximity to each other in parallel molecules, but they are far apart in antiparallel molecules. It seems likely that homologous sequences should be near each other during recombination. Indeed, parallel double crossover molecules have been shown to be meiotic intermediates [26]. We have noted previously that bowtie junctions demonstrate that only the junction need be modified to convert an antiparallel junction to a parallel junction [16].

The work described here redefines the nature of the parallel junction in the same way that previous work [10–15] redefined the antiparallel junction. Neither is ideally parallel or antiparallel in solution, but is distorted from that ideal position by 60–70°; the angle in the crystal structures [13–15] is closer to 40°. Nevertheless, if undistorted by the presence of proteins or other junctions nearby, homologous residues in this type of parallel structure would diverge from each other (in projection) by only 34° from the midline, rather than 60°, as in the antiparallel structure.

The origin of the parallel-like structure for the bowtie junction remains obscure. In both conventional and bowtie junctions, crossover accompanied by chain direction reversal seems to be favored over crossover without reversal. We have shown previously that the origin of this effect in bowtie junctions does not derive from the presence of six internucleotide single bonds in a 5′,5′ linkage, versus four such bonds in a 3′,3′ linkage [16]. In previous work, we have demonstrated that parallel double crossover molecules with parallel helix axes are poorly behaved species, possibly owing to interhelix electrostatic repulsion at strand juxtapositions [23]. However, recent preliminary data (Z. Shen, H. Yan and N.C.S., in preparation), suggest that even strand juxtapositions appear to be favored over non-reversing crossovers. Thus, the non-reversing crossover seems to contain unfavorable structural features that must be overcome to produce parallel structures in conventional junctions.

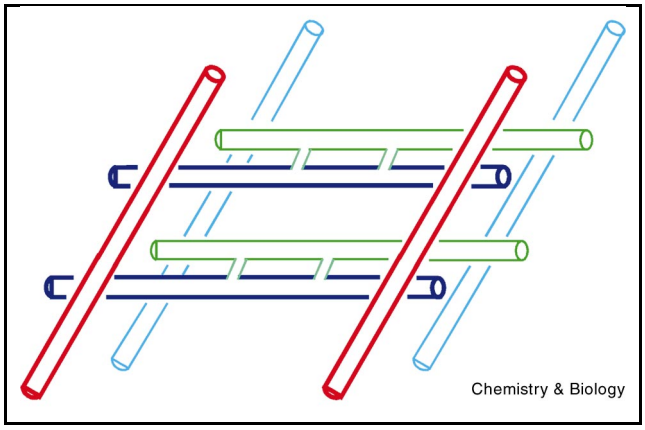

Figure 6. A combined conventional–bowtie parallelogram tile. The conventional parallelogram is closer to the reader, drawn with thicker lines, and the bowtie parallelogram is further from the reader, as indicated by the thin lines. The two parallelograms are connected by double crossover structures. The orientation of the double crossover plane is somewhat arbitrary. The planes here are meant recede from the reader in the order red, dark blue, green, light blue. Note that the inverse relationship in sign between the conventional and bowtie junction enables this structure to be built with the favored structures for each type of junction. In principle, this type of tile could be used to create a space-filling array.

Nanotechnological structures

DNA nanotechnology [27] offers a means of controlling the structure of matter on the nanometer scale. Efforts in this direction have already produced DNA polyhedra [28,29], knots [30], Borromean rings [31], nanomechanical devices [32] and two-dimensional arrays with tunable surface features [18,19] and cavities [12]. It would be desirable to be able to link up the two-dimensional arrays produced by parallelograms [12] in a three-dimensional context, if one could couple them through double crossover structures. Unfortunately, attaching the bottom member of a parallelogram to the top member of another parallelogram reverses the sign of the orientation. This problem could be overcome to produce an authentic three-dimensional tecton by alternating conventional parallelograms with bowtie parallelograms, as shown in Figure 6. Thus, bowtie junctions are likely to prove of value in DNA nanotechnology, as well as serving to explain features of the key Holliday intermediate in recombination.

Significance

The combination of DNA synthetic approaches and AFM can be used to characterize branched DNA structures, such

as Holliday junctions, even when the resolution of the technique appears to be inadequate. This method has been applied to bowtie junctions, which are Holliday junction analogs containing 5′,5′ and 3′,3′ linkages in their crossover strands. Two-dimensional arrays of bowtie junction parallelograms readily provide both the angle between helical domains and its sign through analysis of their AFM images. A series of V-shaped one-dimensional arrays formed from bowtie parallelograms have established the parallel nature of the junctions by AFM.

This work provides further insight into the origins of Holliday junction structure. The bowtie junction is the first Holliday junction analog to demonstrate a preference for the parallel conformation. Long-range electrostatic interactions appear to affect the angle between helices, but the preference for the parallel or antiparallel conformation range seems to be a function of junction structure. In all unrestrained cases examined to date, a structure that reverses chain direction appears favored over one where the strands connecting the helices cross over without reversing direction.

Materials and methods

DNA design, synthesis and purification

All DNA molecules used in this study were designed using the program SEQUIN [33]. The sequences are available as supplementary material. The strands were synthesized on an Applied Biosystems 380B automatic DNA synthesizer, removed from the support, and deprotected using routine phosphoramidite procedures [34]. Strands containing 5′,5′ and 3′,3′ linkages have been synthesized by substituting 5′ phosphoramidites (Glen Research) for conventional 3′ phosphoramidites in half the synthesis. DNA strands have been purified by denaturing gel electrophoresis; bands were cut out of 12–20% denaturing gels and eluted in a solution containing 500 mM ammonium acetate, 10 mM magnesium acetate and 1 mM EDTA.

Formation of hydrogen-bonded complexes and arrays

Complexes were formed by mixing a stoichiometric quantity of each strand (50 nM), as estimated by OD_{260}, in 5 mM HEPES (pH 7.0), 2 mM $MgCl_2$, and 0.5 mM EDTA. This mixture was cooled slowly from 90°C to room temperature in a 1 liter water bath to produce individual parallelograms. The two-dimensional arrays contained only a single parallelogram, so this protocol was sufficient for their production. However, the V-shaped arrays contained several different species. For these arrays, the individual parallelograms were combined in mixtures of I, III and IV or II, III and IV, where the extender parallelograms (III and IV) were in fivefold excess over the fulcrum parallelograms (I or II). These mixtures were then treated to the following thermo-cycling protocol: 26°C, 5 min, 12 cycles of {22°C for 15 min, 19°C, 20 min, 15°C, 30 min}, and 14°C, 1 h. At the completion of this treatment, the samples were visualized on the AFM.

AFM imaging

A 3–5 μl sample drop was spotted on freshly cleaved mica (Ted Pella, Inc.) and left to adsorb to the surface for 2 min. To remove buffer salts, 5–10 drops of double-distilled water were placed on the mica, the drop was shaken off and the sample was dried with compressed air. Imaging was performed in contact mode under isopropanol in a fluid cell on a NanoScope II, using commercial 200 μm cantilevers with Si_3N_4 tips (Digital Instruments). The feedback setpoint was adjusted frequently to minimize the contact force to be approximately 1–5 nN. Similar procedures were used for a control performed on a graphite surface.

Acknowledgements

We would like to thank Chengde Mao for useful discussions. This research has been supported by Grants GM-29554 from the National Institute of General Medical Sciences, N00014-98-1-0093 from the Office of Naval Research, NSF-CCR-97-25021 from the National Science Foundation/DARPA and F30602-98-C-0148 from the Information Directorate of the Air Force Research Laboratory located at Rome, NY.

References

1. Holliday, R. (1964). A mechanism for gene conversion in fungi. *Genet. Res.* **5**, 282–304.
2. Hoess, R., Wierzbicki, A. & Abremski, K. (1987). Characterization of intermediates in site-specific recombination. *Proc. Natl. Acad. Sci. USA* **84**, 6840–6844.
3. Kitts, P.A. & Nash, H.A. (1987). Homology dependent interactions in phage lambda site-specific recombination. *Nature* **329**, 346–348.
4. Nunes-Duby, S.E., Matsumoto, L. & Landy, A. (1987). Site-specific recombination intermediates trapped with suicide substrates. *Cell* **50**, 779–788.
5. Hsieh, P. & Panyutin, I.G. (1995). DNA branch migration. *Nucleic Acids Mol. Biol.* **9**, 42–65.
6. Lilley, D.M.J. & Clegg, R.M. (1993). The structure of the four-way junction in DNA. *Annu. Rev. Biophys. Biomol. Struct.* **22**, 299–328.
7. Seeman, N.C. & Kallenbach, N.R. (1994). DNA branched junctions. *Annu. Rev. Biophys. Biomol. Struct.* **23**, 53–86.
8. Seeman, N.C. (1982). Nucleic acid junctions and lattices. *J. Theor. Biol.* **99**, 237–247.
9. Churchill, M.E.A., Tullius, T.D., Kallenbach, N.R. & Seeman, N.C. (1988). A Holliday recombination intermediate is twofold symmetric. *Proc. Natl. Acad. Sci. USA* **85**, 4653–4656.
10. Murchie, A.I.H., Clegg, R.M., von Kitzing, E., Duckett, D.R., Diekmann, S. & Lilley, D.M.J. (1989). Fluorescence energy transfer shows that the four-way DNA junction is a right-handed cross of antiparallel molecules. *Nature* **341**, 763–766.
11. Eis, P. & Millar, D.P. (1993). Interarm flexibility in a DNA four-way junction revealed by time-resolved fluorescence resonance energy transfer. *Biochemistry* **32**, 13852–13860.
12. Mao, C., Sun, W. & Seeman, N.C. (1999). Designed two-dimensional DNA Holliday junction arrays visualized by atomic force microscopy. *J. Am. Chem. Soc.* **121**, 5437–5443.
13. Ortiz-Lombardia, M., Gonzalez, A., Eritja, R., Aymami, J., Azorin, F. & Coll, M. (1999). *Nature Struct. Biol.* **6**, 913–917.
14. Nowakowski, J., Shim, P.J., Prasad, G.S., Stout, C.D. & Joyce, G.F. (1999). *Nature Struct. Biol.* **6**, 151–156.
15. Eichman, B.F., Vargason, J.M., Mooers, B.H.M. & Ho, P.S. (2000). *Proc. Natl. Acad. Sci. USA* **97**, 3971–3976.
16. Sha, R., Liu, F., Bruist, M.F. & Seeman, N.C. (1999). Parallel helical domains in DNA branched junctions containing 5′,5′ and 3′,3′ linkages. *Biochemistry* **38**, 2832–2841.
17. Cooper, J.P. & Hagerman, P.J. (1987). Gel electrophoretic analysis of the geometry of a DNA four-way junction. *J. Mol. Biol.* **198**, 711–719.
18. Winfree, E., Liu, F., Wenzler, L.A. & Seeman, N.C. (1998). Design and self-assembly of two-dimensional DNA crystals. *Nature* **394**, 539–544.
19. Liu, F., Sha, R. & Seeman, N.C. (1999). Modifying the surface features of two-dimensional DNA crystals. *J. Am. Chem. Soc.* **121**, 917–922.
20. LaBean, T.H., Yan, H., Kopatsch, J., Liu, F., Winfree, E., Reif, J. & Seeman, N.C. (2000). The construction, analysis, ligation and self-assembly of DNA triple crossover molecules. *J. Am. Chem. Soc.* **122**, 1848–1860.
21. Duckett, D.R., Murchie, A.I.H. & Lilley, D.M.J. (1995). *Cell* **83**, 1027–1036.
22. Kimball, A., Guo, Q., Lu, M., Cunningham, R.P., Kallenbach, N.R., Seeman, N.C. & Tullius, T.D. (1990). Conformational isomers of Holliday junctions. *J. Biol. Chem.* **265**, 6544–6547.
23. Fu, T.-J. & Seeman, N.C. (1993). DNA double crossover molecules. *Biochemistry* **32**, 3211–3220.
24. von Kitzing, E., Lilley, D.M.J. & Diekmann, S. (1990). The stereo-

chemistry of DNA four-way junctions, a theoretical study. *Nucleic Acids Res.* **18**, 2671–2683.
25. Seeman, N.C. (1988). Physical models for exploring DNA topology. *J. Biomol. Struct. Dyn.* **5**, 997–1004.
26. Schwacha, A. & Kleckner, N. (1995). Identification of double Holliday junctions as intermediates in meiotic recombination. *Cell* **83**, 783–791.
27. Seeman, N.C. (1998). DNA nanotechnology: Novel DNA constructions. *Annu. Rev. Biophys. Biomol. Struct.* **27**, 225–248.
28. Chen, J. & Seeman, N.C. (1991). The synthesis from DNA of a molecule with the connectivity of a cube. *Nature* **350**, 631–633.
29. Zhang, Y. & Seeman, N.C. (1994). The construction of a DNA truncated octahedron. *J. Am. Chem. Soc.* **116**, 1661–1669.
30. Mueller, J.E., Du, S.M. & Seeman, N.C. (1991). The design and synthesis of a knot from single-stranded DNA. *J. Am. Chem. Soc.* **113**, 6306–6308.
31. Mao, C., Sun, W. & Seeman, N.C. (1997). Assembly of Borromean rings from DNA. *Nature* **386**, 137–138.
32. Mao, C., Sun, W., Shen, Z. & Seeman, N.C. (1999). A DNA nanomechanical device based on the B-Z transition. *Nature* **397**, 144–146.
33. Seeman, N.C. (1990). De novo design of sequences for nucleic acid structure engineering. *J. Biomol. Struct. Dyn.* **8**, 573–581.
34. Caruthers, M.H. (1985). Gene synthesis machines: DNA chemistry and its uses. *Science* **230**, 281–285.